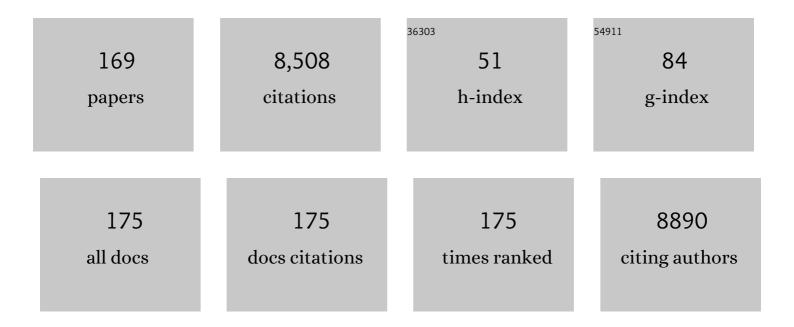
## Mingdeng Wei

List of Publications by Year in descending order

Source: https://exaly.com/author-pdf/9343969/publications.pdf Version: 2024-02-01



#	Article	IF	CITATIONS
1	Tin-based metal-phosphine complexes nanoparticles as long-cycle life electrodes for high-performance hybrid supercapacitors. Journal of Colloid and Interface Science, 2022, 606, 148-157.	9.4	8
2	Defect passivation of a perovskite film by ZnIn <sub>2</sub> S <sub>4</sub> nanosheets for efficient and stable perovskite solar cells. Chemical Communications, 2022, 58, 653-656.	4.1	4
3	Two-dimentional MoSe2/chitosan-derived nitrogen-doped carbon composite enabling stable sodium/potassium storage. Journal of Physics and Chemistry of Solids, 2022, 163, 110573.	4.0	7
4	Structural engineering of tin sulfides anchored on nitrogen/phosphorus dual-doped carbon nanofibres in sodium/potassium-ion batteries. Carbon, 2022, 189, 46-56.	10.3	86
5	Selfâ€Optimizing Effect in Lithium Storage of GeO <sub>2</sub> Induced by Heterointerface Regulation. Small, 2022, 18, e2106067.	10.0	5
6	Structure Engineering of BiSbS <sub><i>x</i></sub> Nanocrystals Embedded within Sulfurized Polyacrylonitrile Fibers for High Performance of Potassiumâ€Ion Batteries. Chemistry - A European Journal, 2022, 28, .	3.3	5
7	Realizing reversible conversion-alloying of GeO2/N-doped carbon nanocomposite with oxygen vacancies for lithium-ion batteries. Materials Today Nano, 2022, 18, 100196.	4.6	2
8	A composite of two dimensional GeSe2/nitrogenâ€doped reduced graphene oxide for enhanced capacitive lithiumâ€ion storage. Chemistry - A European Journal, 2022, , .	3.3	2
9	Dual-carbon materials coated Ge/Si composite for high performance lithium-ion batteries. Electrochimica Acta, 2022, 417, 140337.	5.2	8
10	A General Synthesis of Mesoporous Hollow Carbon Spheres with Extraordinary Sodium Storage Kinetics by Engineering Solvation Structure. Small, 2022, 18, e2106513.	10.0	4
11	Stabilizing intermediate phases <i>via</i> the efficient confinement effects of the SnS <sub>2</sub> -SPAN fibre composite for ultra-stable half/full sodium/potassium-ion batteries. Journal of Materials Chemistry A, 2022, 10, 11449-11457.	10.3	36
12	Highâ€Rate, Large Capacity, and Long Life Dendriteâ€Free Zn Metal Anode Enabled by Trifunctional Electrolyte Additive with a Wide Temperature Range. Advanced Science, 2022, 9, .	11.2	91
13	lonic Liquidâ€Assisted Crystallization and Defect Passivation for Efficient Perovskite Solar Cells with Enhanced Open ircuit Voltage. ChemSusChem, 2022, 15, .	6.8	14
14	Conductive-free Zn2GeO4@multi-walled carbon nanotubes for high-performance lithium-ion storage. Journal of Alloys and Compounds, 2022, , 165720.	5.5	1
15	The optimized interface engineering of VS2 as cathodes for high performance all-solid-state lithium-ion battery. Science China Technological Sciences, 2022, 65, 1859-1866.	4.0	11
16	Construction of FeS2@C coated with reduced graphene oxide as high-performance anode for lithium-ion batteries. Journal of Electroanalytical Chemistry, 2022, 918, 116467.	3.8	4
17	High stability and high performance nitrogen doped carbon containers for lithium-ion batteries. Journal of Colloid and Interface Science, 2022, 625, 692-699.	9.4	3
18	In situ simultaneous encapsulation of defective MoS2 nanolayers and sulfur nanodots into SPAN fibers for high rate sodium-ion batteries. Chemical Engineering Journal, 2021, 404, 126430.	12.7	90

#	Article	IF	CITATIONS
19	General Synthesis of Sulfonateâ€Based Metal–Organic Framework Derived Composite of M <sub><i>x</i></sub> S <sub><i>y</i></sub> @N/Sâ€Doped Carbon for Highâ€Performance Lithium/Sodium Ion Batteries. Chemistry - A European Journal, 2021, 27, 2104-2111.	3.3	23
20	Dual carbon decorated germanium-carbon composite as a stable anode for sodium/potassium-ion batteries. Journal of Colloid and Interface Science, 2021, 584, 372-381.	9.4	30
21	Hierarchical structure TiNb <sub>2</sub> O <sub>7</sub> microspheres derived from titanate for high-performance lithium-ion batteries. CrystEngComm, 2021, 23, 4905-4909.	2.6	5
22	N-Doped carbon encapsulating Bi nanoparticles derived from metal–organic frameworks for high-performance sodium-ion batteries. Journal of Materials Chemistry A, 2021, 9, 22048-22055.	10.3	33
23	Facile fabrication of WS <sub>2</sub> nanocrystals confined in chlorella-derived N, P co-doped bio-carbon for sodium-ion batteries with ultra-long lifespan. Dalton Transactions, 2021, 50, 14745-14752.	3.3	6
24	A thioacetamide interlayer anchoring TiO 2 and (FAPbI 3 ) 1â^' x (MAPbBr 3 ) x for highâ€performance perovskite solar cells. Journal of the American Ceramic Society, 2021, 104, 5120-5126.	3.8	2
25	Template-free fabrication of 1D core-shell MoO2@MoS2/nitrogen-doped carbon nanorods for enhanced lithium/sodium-ion storage. Journal of Colloid and Interface Science, 2021, 588, 804-812.	9.4	28
26	Preparation of SnS2/enteromorpha prolifera derived carbon composite and its performance of sodium-ion batteries. Journal of Physics and Chemistry of Solids, 2021, 152, 109976.	4.0	9
27	Nanocomposite of ultra-small MoO2 embedded in nitrogen-doped carbon: In situ derivation from an organic molybdenum complex and its superior Li-Ion storage performance. Journal of Colloid and Interface Science, 2021, 592, 33-41.	9.4	22
28	In situ synthesis of g-C3N4 by glass-assisted annealing route to boost the efficiency of perovskite solar cells. Journal of Colloid and Interface Science, 2021, 591, 326-333.	9.4	17
29	Nitrogen-doped carbon encapsulated zinc vanadate polyhedron engineered from a metal–organic framework as a stable anode for alkali ion batteries. Journal of Colloid and Interface Science, 2021, 593, 251-265.	9.4	33
30	Inâ€Situ Growth Mirrorâ€Like Cobalt Sulfide Nanosheets on ITO for High Efficiency Counter Electrode of Dyeâ€Sensitized Solar Cells**. ChemistrySelect, 2021, 6, 7537-7541.	1.5	2
31	Algal residues-engaged formation of novel WVO4/V3Se4 hybrid nanostructure with carbon fiber confinement for enhanced long-term cycling stability in sodium/potassium storage. Journal of Alloys and Compounds, 2021, 892, 162177.	5.5	6
32	V3Se4 embedded within N/P co-doped carbon fibers for sodium/potassium ion batteries. Chemical Engineering Journal, 2021, 419, 129607.	12.7	89
33	Dual-phase TiO2 hollow microspheres as a superior anode for sodium ion battery. Journal of Electroanalytical Chemistry, 2021, 899, 115687.	3.8	2
34	Open-framework germanates derived GeO2/C nanocomposite as a long-life and high-capacity anode for lithium-ion batteries. Journal of Alloys and Compounds, 2021, 881, 160533.	5.5	9
35	Low crystalline 1T-MoS2@S-doped carbon hollow spheres as an anode material for Lithium-ion battery. Journal of Colloid and Interface Science, 2021, 601, 411-417.	9.4	21
36	A new neodymium–phosphine compound for supercapacitors with long-term cycling stability. Chemical Communications, 2021, 57, 5933-5936.	4.1	4

#	Article	IF	CITATIONS
37	Stable Li-ion storage in Ge/N-doped carbon microsphere anodes. Nanoscale, 2021, 13, 5307-5315.	5.6	7
38	Co-construction of sulfur vacancies and carbon confinement in V <sub>5</sub> S <sub>8</sub> /CNFs to induce an ultra-stable performance for half/full sodium-ion and potassium-ion batteries. Nanoscale, 2021, 13, 5033-5044.	5.6	90
39	D–A–π–A organic sensitizer surface passivation for efficient and stable perovskite solar cells. Journal of Materials Chemistry A, 2021, 9, 25086-25093.	10.3	28
40	In situ fabrication of ZnO–MoO2/C hetero-phase nanocomposite derived from MOFs with enhanced performance for lithium storage. Journal of Alloys and Compounds, 2020, 817, 152728.	5.5	14
41	A composite of ultra-fine few-layer MoS <sub>2</sub> structures embedded on N,P-co-doped bio-carbon for high-performance sodium-ion batteries. New Journal of Chemistry, 2020, 44, 2046-2052.	2.8	6
42	A new promising Ni-MOF superstructure for high-performance supercapacitors. Chemical Communications, 2020, 56, 1803-1806.	4.1	93
43	In Situ Confined Co5Ge3 Alloy Nanoparticles in Nitrogen-Doped Carbon Nanotubes for Boosting Lithium Storage. ACS Applied Materials & Interfaces, 2020, 12, 46247-46253.	8.0	11
44	Synthesis of the Se-HPCF composite <i>via</i> a liquid-solution route and its stable cycling performance in Li–Se batteries. Dalton Transactions, 2020, 49, 14536-14542.	3.3	5
45	TiO <sub>2</sub> Mesocrystals Processed at Low Temperature as the Electronâ€Transport Material in Perovskite Solar Cells. ChemSusChem, 2020, 13, 5256-5263.	6.8	7
46	Cu2S hollow spheres as an anode for high-rate sodium storage performance. Journal of Electroanalytical Chemistry, 2020, 874, 114523.	3.8	20
47	Rational Design of Hierarchical SnS <sub>2</sub> Microspheres with S Vacancy for Enhanced Sodium Storage Performance. ACS Sustainable Chemistry and Engineering, 2020, 8, 9519-9525.	6.7	52
48	High-Performance Lithium-Ion-Based Dual-Ion Batteries Enabled by Few-Layer MoSe <sub>2</sub> /Nitrogen-Doped Carbon. ACS Sustainable Chemistry and Engineering, 2020, 8, 5514-5523.	6.7	37
49	Hierarchical Porous Anatase TiO2 Microspheres with High-Rate and Long-Term Cycling Stability for Sodium Storage in Ether-Based Electrolyte. ACS Applied Energy Materials, 2020, 3, 3619-3627.	5.1	13
50	Metal–organic framework-derived hollow structure CoS <sub>2</sub> /nitrogen-doped carbon spheres for high-performance lithium/sodium ion batteries. Chemical Communications, 2020, 56, 3951-3954.	4.1	35
51	SnS2 nanosheets anchored on porous carbon fibers for high performance of sodium-ion batteries. Journal of Electroanalytical Chemistry, 2020, 862, 114021.	3.8	14
52	Biological impact of lead from halide perovskites reveals the risk of introducing a safe threshold. Nature Communications, 2020, 11, 310.	12.8	313
53	In situ fabrication of ultrathin few-layered WSe2 anchored on N, P dual-doped carbon by bioreactor for half/full sodium/potassium-ion batteries with ultralong cycling lifespan. Journal of Colloid and Interface Science, 2020, 574, 217-228.	9.4	67
54	Facile fabrication of a vanadium nitride/carbon fiber composite for half/full sodium-ion and potassium-ion batteries with long-term cycling performance. Nanoscale, 2020, 12, 10693-10702.	5.6	39

#	Article	IF	CITATIONS
55	Enhanced Performance of Sn-Based Perovskite Solar Cells by Two-Dimensional Perovskite Doping. ACS Sustainable Chemistry and Engineering, 2020, 8, 8624-8628.	6.7	31
56	An inorganic stable Sn-based perovskite film with regulated nucleation for solar cell application. Journal of Materials Chemistry C, 2020, 8, 8840-8845.	5.5	27
57	Facile Synthesis of Ultra‧mall Few‣ayer Nanostructured MoSe <sub>2</sub> Embedded on N, P Coâ€Đoped Bio arbon for Highâ€Performance Half/Full Sodiumâ€ŀon and Potassiumâ€ŀon Batteries. Chemistry A European Journal, 2019, 25, 13411-13421.	-3.3	61
58	Facile synthesis of VN hollow spheres as an anode for lithium-ion battery. Journal of Electroanalytical Chemistry, 2019, 848, 113360.	3.8	20
59	Synthesis of anatase TiO2 mesocrystals with highly exposed low-index facets for enhanced electrochemical performance. Electrochimica Acta, 2019, 319, 101-109.	5.2	15
60	Electrospun VSe <sub>1.5</sub> /CNF composite with excellent performance for alkali metal ion batteries. Nanoscale, 2019, 11, 16308-16316.	5.6	50
61	Highly Efficient Perovskite Solar Cells Based on a Zn <sub>2</sub> SnO <sub>4</sub> Compact Layer. ACS Applied Materials & Interfaces, 2019, 11, 36553-36559.	8.0	34
62	Template-free synthesis of metallic WS2 hollow microspheres as an anode for the sodium-ion battery. Journal of Colloid and Interface Science, 2019, 557, 722-728.	9.4	31
63	An ultra-small few-layer MoS2-hierarchical porous carbon fiber composite obtained via nanocasting synthesis for sodium-ion battery anodes with excellent long-term cycling performance. Dalton Transactions, 2019, 48, 4149-4156.	3.3	44
64	TiO2-B as an electron transporting material for highly efficient perovskite solar cells. Journal of Power Sources, 2019, 415, 8-14.	7.8	33
65	Reversible conversion reaction of GeO <sub>2</sub> boosts lithium-ion storage <i>via</i> Fe doping. Journal of Materials Chemistry A, 2019, 7, 4574-4580.	10.3	34
66	TiO <sub>2</sub> -B nanowires <i>via</i> topological conversion with enhanced lithium-ion intercalation properties. Journal of Materials Chemistry A, 2019, 7, 3842-3847.	10.3	37
67	Hierarchical spheres constructed by ultrathin VS <sub>2</sub> nanosheets for sodium-ion batteries. Journal of Materials Chemistry A, 2019, 7, 3691-3696.	10.3	94
68	Preparation of Ge/N, S co-doped ordered mesoporous carbon composite and its long-term cycling performance of lithium-ion batteries. Electrochimica Acta, 2019, 318, 737-745.	5.2	26
69	Sulfur-Doped Anatase TiO <sub>2</sub> as an Anode for High-Performance Sodium-Ion Batteries. ACS Applied Energy Materials, 2019, 2, 3791-3797.	5.1	46
70	Nanocomposite of Mo <sub>2</sub> N Quantum Dots@MoO <sub>3</sub> @Nitrogen-Doped Carbon as a High-Performance Anode for Lithium-Ion Batteries. ACS Sustainable Chemistry and Engineering, 2019, 7, 10198-10206.	6.7	30
71	Valence Engineering via Selective Atomic Substitution on Tetrahedral Sites in Spinel Oxide for Highly Enhanced Oxygen Evolution Catalysis. Journal of the American Chemical Society, 2019, 141, 8136-8145.	13.7	220
72	Efficient Dye-Sensitized Solar Cells Composed of Nanostructural ZnO Doped with Ti. Catalysts, 2019, 9, 273.	3.5	34

#	Article	IF	CITATIONS
73	Hollow SiO2 microspheres coated with nitrogen doped carbon layer as an anode for high performance lithium-ion batteries. Electrochimica Acta, 2019, 306, 106-112.	5.2	51
74	Co <sub>9</sub> S <sub>8</sub> embedded into N/S doped carbon composites: <i>in situ</i> derivation from a sulfonate-based metal–organic framework and its electrochemical properties. Journal of Materials Chemistry A, 2019, 7, 10331-10337.	10.3	75
75	Rational design of few-layer MoSe <sub>2</sub> confined within ZnSe–C hollow porous spheres for high-performance lithium-ion and sodium-ion batteries. Nanoscale, 2019, 11, 6766-6775.	5.6	143
76	MoS2 hollow spheres in ether-based electrolyte for high performance sodium ion battery. Journal of Colloid and Interface Science, 2019, 548, 20-24.	9.4	40
77	Realization of ultra-long columnar single crystals in TiO <sub>2</sub> nanotube arrays as fast electron transport channels for high efficiency dye-sensitized solar cells. Journal of Materials Chemistry A, 2019, 7, 11520-11529.	10.3	19
78	ZnO nanosheets encapsulating graphene quantum dots with enhanced performance for dye-sensitized solar cell. Journal of Electroanalytical Chemistry, 2019, 840, 160-164.	3.8	13
79	An Sn doped 1T–2H MoS <sub>2</sub> few-layer structure embedded in N/P co-doped bio-carbon for high performance sodium-ion batteries. Chemical Communications, 2019, 55, 3614-3617.	4.1	69
80	Fabrication of Zn2SnO4 microspheres with controllable shell numbers for highly efficient dye-sensitized solar cells. Solar Energy, 2019, 181, 424-429.	6.1	25
81	Hierarchical Composite of Roseâ€Like VS <sub>2</sub> @S/Nâ€Doped Carbon with Expanded (001) Planes for Superior Liâ€Ion Storage. Small, 2019, 15, e1903904.	10.0	64
82	Highly efficient Zn2SnO4 perovskite solar cells through band alignment engineering. Chemical Communications, 2019, 55, 14673-14676.	4.1	18
83	A hierarchical composite of GeO <sub>2</sub> nanotubes/N-doped carbon microspheres with high-rate and super-durable performance for lithium-ion batteries. Chemical Communications, 2019, 55, 14319-14322.	4.1	14
84	Facile synthesis of hierarchical lychee-like Zn3V3O8@C/rGO nanospheres as high-performance anodes for lithium ion batteries. Journal of Colloid and Interface Science, 2019, 533, 627-635.	9.4	33
85	Hierarchically structural Ge encapsulated with nitrogen-doped carbon for high performance lithium storage. Journal of Electroanalytical Chemistry, 2019, 832, 182-188.	3.8	6
86	Two-dimensional MoN@N-doped carbon hollow spheres as an anode material for high performance lithium-ion battery. Electrochimica Acta, 2019, 295, 246-252.	5.2	39
87	In situ synthesis of Mn3O4 on Ni foam/graphene substrate as a newly self-supported electrode for high supercapacitive performance. Journal of Colloid and Interface Science, 2019, 534, 665-671.	9.4	26
88	Plasmonic Effects of Silver Nanoparticles Embedded in the Counter Electrode on the Enhanced Performance of Dye-Sensitized Solar Cells. Langmuir, 2018, 34, 5367-5373.	3.5	20
89	Synthesis of hierarchically mesoporous TiO2 spheres via a emulsion polymerization route for superior lithium-ion batteries. Journal of Electroanalytical Chemistry, 2018, 818, 1-9.	3.8	14
90	Metal–organic frameworks at interfaces of hybrid perovskite solar cells for enhanced photovoltaic properties. Chemical Communications, 2018, 54, 1253-1256.	4.1	106

#	Article	IF	CITATIONS
91	Anatase TiO <sub>2</sub> Quantum Dots with a Narrow Band Gap of 2.85 eV Based on Surface Hydroxyl Groups Exhibiting Significant Photodegradation Property. European Journal of Inorganic Chemistry, 2018, 2018, 1506-1510.	2.0	20
92	In Situ Synthesis of WSe <sub>2</sub> /CMK-5 Nanocomposite for Rechargeable Lithium-Ion Batteries with a Long-Term Cycling Stability. ACS Sustainable Chemistry and Engineering, 2018, 6, 4688-4694.	6.7	47
93	Preparation of a Si/SiO <sub>2</sub> –Orderedâ€Mesoporousâ€Carbon Nanocomposite as an Anode for Highâ€Performance Lithiumâ€Ion and Sodiumâ€Ion Batteries. Chemistry - A European Journal, 2018, 24, 4841-4848.	3.3	70
94	Hierarchical TiO <sub>2â^'x</sub> imbedded with graphene quantum dots for high-performance lithium storage. Chemical Communications, 2018, 54, 1413-1416.	4.1	60
95	Rapid and facile synthesis of hierarchically mesoporous TiO <sub>2</sub> –B with enhanced reversible capacity and rate capability. Journal of Materials Chemistry A, 2018, 6, 1196-1200.	10.3	34
96	Highly Efficient Perovskite Solar Cells Based on Zn <sub>2</sub> Ti <sub>3</sub> O <sub>8</sub> Nanoparticles as Electron Transport Material. ChemSusChem, 2018, 11, 424-431.	6.8	17
97	Graphene quantum dots decorated TiO2 mesoporous film as an efficient electron transport layer for high-performance perovskite solar cells. Journal of Power Sources, 2018, 402, 320-326.	7.8	86
98	Highly Efficient Degradation of Tobacco Specific Nâ€Nitrosamines by TiO <sub>2</sub> Mesocrystals with Robust and Tailored Microporous Structure. ChemistrySelect, 2018, 3, 10266-10270.	1.5	0
99	Covering effect of conductive glass: a facile route to tailor the grain growth of hybrid perovskites for highly efficient solar cells. Journal of Materials Chemistry A, 2018, 6, 20289-20296.	10.3	10
100	Brookite TiO <sub>2</sub> mesocrystals with enhanced lithium-ion intercalation properties. Chemical Communications, 2018, 54, 11491-11494.	4.1	33
101	Rational Design and General Synthesis of Sâ€Doped Hard Carbon with Tunable Doping Sites toward Excellent Naâ€Ion Storage Performance. Advanced Materials, 2018, 30, e1802035.	21.0	239
102	Hierarchical Cobaltâ€Based Metal–Organic Framework for Highâ€Performance Lithiumâ€lon Batteries. Chemistry - A European Journal, 2018, 24, 13362-13367.	3.3	60
103	Facile Deposition of Nb <sub>2</sub> O <sub>5</sub> Thin Film as an Electron-Transporting Layer for Highly Efficient Perovskite Solar Cells. ACS Applied Nano Materials, 2018, 1, 4101-4109.	5.0	33
104	Hierarchical TiO2-B composed of nanosheets with exposed {010} facets as a high-performance anode for lithium ion batteries. Journal of Power Sources, 2018, 392, 226-231.	7.8	29
105	A one-step synthesis of porous V <sub>2</sub> O <sub>3</sub> @C hollow spheres as a high-performance anode for lithium-ion batteries. Chemical Communications, 2018, 54, 7346-7349.	4.1	59
106	Rutile TiO 2 mesocrystals with tunable subunits as a long-term cycling performance anode for sodium-ion batteries. Journal of Alloys and Compounds, 2017, 699, 455-462.	5.5	19
107	Nbâ€Doped Rutile TiO <sub>2</sub> Mesocrystals with Enhanced Lithium Storage Properties for Lithium Ion Battery. Chemistry - A European Journal, 2017, 23, 5059-5065.	3.3	39
108	Facile preparation of a V <sub>2</sub> O <sub>3</sub> /carbon fiber composite and its application for long-term performance lithium-ion batteries. New Journal of Chemistry, 2017, 41, 5380-5386.	2.8	29

#	Article	IF	CITATIONS
109	Bis(phenothiazylâ€ethynylene)â€Based Organic Dyes Containing Diâ€Anchoring Groups with Efficiency Comparable to N719 for Dyeâ€Sensitized Solar Cells. Chemistry - an Asian Journal, 2017, 12, 332-340.	3.3	9
110	Carbon coated anatase TiO 2 mesocrystals enabling ultrastable and robust sodium storage. Journal of Power Sources, 2017, 359, 64-70.	7.8	47
111	Green synthesis of a Se/HPCF–rGO composite for Li–Se batteries with excellent long-term cycling performance. Journal of Materials Chemistry A, 2017, 5, 22997-23005.	10.3	61
112	Rutile TiO <sub>2</sub> Mesocrystals as Sulfur Host for Highâ€Performance Lithium–Sulfur Batteries. Chemistry - A European Journal, 2017, 23, 16312-16318.	3.3	36
113	Heterogeneous TiO2@Nb2O5 composite as a high-performance anode for lithium-ion batteries. Scientific Reports, 2017, 7, 7204.	3.3	10
114	A multi-functional gum arabic binder for NiFe <sub>2</sub> O <sub>4</sub> nanotube anodes enabling excellent Li/Na-ion storage performance. Journal of Materials Chemistry A, 2017, 5, 18138-18147.	10.3	35
115	A CMK-5-encapsulated MoSe <sub>2</sub> composite for rechargeable lithium-ion batteries with improved electrochemical performance. Journal of Materials Chemistry A, 2017, 5, 19632-19638.	10.3	85
116	Synthesis of Mesoporous Co <sup>2+</sup> -Doped TiO <sub>2</sub> Nanodisks Derived from Metal Organic Frameworks with Improved Sodium Storage Performance. ACS Applied Materials & Interfaces, 2017, 9, 32071-32079.	8.0	64
117	Layered Structural Coâ€Based MOF with Conductive Network Frames as a New Supercapacitor Electrode. Chemistry - A European Journal, 2017, 23, 631-636.	3.3	257
118	An in situ formed Se/CMK-3 composite for rechargeable lithium-ion batteries with long-term cycling performance. Journal of Materials Chemistry A, 2016, 4, 13646-13651.	10.3	54
119	Hierarchical MoS2@RGO nanosheets for high performance sodium storage. Journal of Power Sources, 2016, 331, 50-57.	7.8	92
120	Nitrogen-doped carbon coated silicon derived from a facile strategy with enhanced performance for lithium storage. Functional Materials Letters, 2016, 09, 1650055.	1.2	6
121	Hierarchical cerium oxide derived from metal-organic frameworks for high performance supercapacitor electrodes. Electrochimica Acta, 2016, 222, 773-780.	5.2	120
122	Ethanol thermal reduction synthesis of hierarchical MoO <sub>2</sub> –C hollow spheres with high rate performance for lithium ion batteries. RSC Advances, 2016, 6, 105558-105564.	3.6	33
123	Improving the efficiency of dye-sensitized solar cells by photoanode surface modifications. Science China Materials, 2016, 59, 867-883.	6.3	13
124	Ge/GeO <sub>2</sub> -Ordered Mesoporous Carbon Nanocomposite for Rechargeable Lithium-Ion Batteries with a Long-Term Cycling Performance. ACS Applied Materials & Interfaces, 2016, 8, 232-239.	8.0	88
125	Metal–Organic Framework Derived Hierarchical Porous Anatase TiO <sub>2</sub> as a Photoanode for Dye-Sensitized Solar Cell. Crystal Growth and Design, 2016, 16, 121-125.	3.0	68
126	Rutile TiO2 Mesocrystals/Reduced Graphene Oxide with High-Rate and Long-Term Performance for Lithium-Ion Batteries. Scientific Reports, 2015, 5, 8498.	3.3	46

#	Article	IF	CITATIONS
127	In situ synthesis of GeO <sub>2</sub> /reduced graphene oxide composite on Ni foam substrate as a binder-free anode for high-capacity lithium-ion batteries. Journal of Materials Chemistry A, 2015, 3, 1619-1623.	10.3	83
128	Recent Progress in Preparation and Lithiumâ€ion Storage Properties of TiO <sub>2</sub> Mesocrystals. Journal of the Chinese Chemical Society, 2015, 62, 209-216.	1.4	5
129	One-step hydrothermal synthesis of Nb doped brookite TiO <sub>2</sub> nanosheets with enhanced lithium-ion intercalation properties. Journal of Materials Chemistry A, 2015, 3, 18882-18888.	10.3	30
130	Facile synthesis of rutile TiO <sub>2</sub> mesocrystals with enhanced sodium storage properties. Journal of Materials Chemistry A, 2015, 3, 17412-17416.	10.3	80
131	Iso-Oriented Anatase TiO2 Mesocages as a High Performance Anode Material for Sodium-Ion Storage. Scientific Reports, 2015, 5, 11960.	3.3	66
132	Nanocomposite Li <sub>3</sub> V <sub>2</sub> (PO <sub>4</sub> ) <sub>3</sub> /carbon as a cathode material with high rate performance and long-term cycling stability in lithium-ion batteries. RSC Advances, 2015, 5, 57127-57132.	3.6	13
133	ZnO nanowires array grown on Ga-doped ZnO single crystal for dye-sensitized solar cells. Scientific Reports, 2015, 5, 11499.	3.3	18
134	Hierarchical LiZnVO <sub>4</sub> @C nanostructures with enhanced cycling stability for lithium-ion batteries. Dalton Transactions, 2015, 44, 7967-7972.	3.3	20
135	Ultrathin TiO2-B nanowires with enhanced electrochemical performance for Li-ion batteries. Journal of Materials Chemistry A, 2015, 3, 10038-10044.	10.3	37
136	Composite of K-doped (NH <sub>4</sub> ) <sub>2</sub> V <sub>3</sub> O <sub>8</sub> /graphene as an anode material for sodium-ion batteries. Dalton Transactions, 2015, 44, 18864-18869.	3.3	19
137	Synthesis of hierarchical ZnV <sub>2</sub> O <sub>4</sub> microspheres and its electrochemical properties. CrystEngComm, 2014, 16, 10309-10313.	2.6	48
138	Ultrasensitive electrochemical sensor for p-nitrophenyl organophosphates based on ordered mesoporous carbons at low potential without deoxygenization. Analytica Chimica Acta, 2014, 822, 23-29.	5.4	41
139	Enhanced electrochemical performance of ammonium vanadium bronze through sodium cation intercalation and optimization of electrolyte. Journal of Colloid and Interface Science, 2014, 418, 273-276.	9.4	15
140	Facile synthesis of V6O13 micro-flowers for Li-ion and Na-ion battery cathodes with good cycling performance. Journal of Colloid and Interface Science, 2014, 425, 1-4.	9.4	55
141	Hierarchically porous TiO <sub>2</sub> microspheres as a high performance anode for lithium-ion batteries. Journal of Materials Chemistry A, 2014, 2, 1102-1106.	10.3	72
142	Understanding the growth and photoelectrochemical properties of mesocrystals and single crystals: a case of anatase TiO <sub>2</sub> . Physical Chemistry Chemical Physics, 2014, 16, 7441-7447.	2.8	14
143	Efficiency enhanced dye-sensitized Zn <sub>2</sub> SnO <sub>4</sub> solar cells using a facile chemical-bath deposition method. New Journal of Chemistry, 2014, 38, 4465.	2.8	28
144	Zn-doped Ni-MOF material with a high supercapacitive performance. Journal of Materials Chemistry A, 2014, 2, 19005-19010.	10.3	395

#	Article	IF	CITATIONS
145	Facile synthesis of Li <sub>2</sub> MnO <sub>3</sub> nanowires for lithium-ion battery cathodes. New Journal of Chemistry, 2014, 38, 584-587.	2.8	22
146	Hierarchically porous anatase TiO <sub>2</sub> microspheres composed of tiny octahedra with enhanced electrochemical properties in lithium-ion batteries. Journal of Materials Chemistry A, 2014, 2, 20133-20138.	10.3	34
147	Metal–organic frameworks: a new promising class of materials for a high performance supercapacitor electrode. Journal of Materials Chemistry A, 2014, 2, 16640-16644.	10.3	505
148	Metal–Organic Frameworks at Interfaces in Dye‣ensitized Solar Cells. ChemSusChem, 2014, 7, 2469-2472.	6.8	57
149	Facile synthesis of hierarchical MnO2 sub-microspheres composed of nanosheets and their application for supercapacitors. RSC Advances, 2014, 4, 40753-40757.	3.6	35
150	Sensitive electrochemical microbial biosensor for p-nitrophenylorganophosphates based on electrode modified with cell surface-displayed organophosphorus hydrolase and ordered mesopore carbons. Biosensors and Bioelectronics, 2014, 60, 137-142.	10.1	67
151	Facile synthesis of ammonium vanadium oxide nanorods for Na-ion battery cathodes. Journal of Colloid and Interface Science, 2014, 428, 73-77.	9.4	34
152	Composites of V2O3–ordered mesoporous carbon as anode materials for lithium-ion batteries. Carbon, 2013, 62, 382-388.	10.3	89
153	Ordered mesoporous TiO2–C nanocomposite as an anode material for long-term performance lithium-ion batteries. Journal of Materials Chemistry A, 2013, 1, 4293.	10.3	111
154	Synthesis of TiO2 nanoparticles with tunable dominant exposed facets (010), (001) and (106). CrystEngComm, 2013, 15, 3040.	2.6	21
155	Layered titanate nanostructures and their derivatives as negative electrode materials for lithium-ion batteries. Journal of Materials Chemistry A, 2013, 1, 4403.	10.3	84
156	MoO <sub>2</sub> -Ordered Mesoporous Carbon Nanocomposite as an Anode Material for Lithium-Ion Batteries. ACS Applied Materials & Interfaces, 2013, 5, 2182-2187.	8.0	138
157	Layered H <sub>2</sub> Ti <sub>6</sub> O <sub>13</sub> â€Nanowires: A New Promising Pseudocapacitive Material in Nonâ€Aqueous Electrolyte. Advanced Functional Materials, 2012, 22, 5185-5193.	14.9	213
158	Flexible dye-sensitized ZnO quantum dots solar cells. RSC Advances, 2012, 2, 9565.	3.6	20
159	ZnV2O4–CMK nanocomposite as an anode material for rechargeable lithium-ion batteries. Journal of Materials Chemistry, 2012, 22, 14284.	6.7	67
160	Self-assembled nanoporous rutile TiO2 mesocrystals with tunable morphologies for high rate lithium-ion batteries. Nano Energy, 2012, 1, 466-471.	16.0	97
161	Additive-free synthesis of unique TiO <sub>2</sub> mesocrystals with enhanced lithium-ion intercalation properties. Energy and Environmental Science, 2012, 5, 5408-5413.	30.8	145
162	Metal–organic frameworks: Promising materials for enhancing electrochemical properties of nanostructured Zn2SnO4 anode in Li-ion batteries. CrystEngComm, 2012, 14, 2112.	2.6	56

#	Article	IF	CITATIONS
163	Metal platinum-wrapped mesoporous carbon for sensitive electrochemical immunosensing based on cyclodextrin functionalized graphene nanosheets. Electrochimica Acta, 2012, 68, 158-165.	5.2	37
164	Complex spinel titanate nanowires for a high rate lithium-ion battery. Energy and Environmental Science, 2011, 4, 1886.	30.8	115
165	Metal–organic frameworks: promising materials for improving the open circuit voltage of dye-sensitized solar cells. Journal of Materials Chemistry, 2011, 21, 17259.	6.7	176
166	ULTRATHIN <font>Li</font> <sub>4</sub> <font>Ti</font> <sub>5</sub> <font>O</font> <sub>12</sub> NANOSHEETS AS A HIGH PERFORMANCE ANODE FOR <font>Li</font> -ION BATTERY. Functional Materials Letters, 2011, 04, 389-393.	1.2	28
167	SPINEL <font>Li<sub>2</sub>MTi<sub>3</sub>O<sub>8</sub></font> ( <font>M = Mg,) Tj ETQq1 1 0.784314 r STORAGE. Functional Materials Letters, 2011, 04, 65-69.</font>	gBT /Over 1.2	lock 10 Tf 50 46
168	Selective Synthesis of Rutile, Anatase, and Brookite Nanorods by a Hydrothermal Route. Current Nanoscience, 2010, 6, 479-482.	1.2	18
169	Synthesis and characterization of nanosheet-shaped titanium dioxide. Journal of Materials Science, 2007, 42, 529-533.	3.7	31